Line Profiles of Ni-like Collisional XUV Laser Amplifiers: Particle Correlation Effects

Annette Calisti, Sandrine Ferri, Caroline Mossé, Bernard Talin, Annie Klisnick, Limin Meng, Djamel Benredjem, Olivier Guilbaud

▶ **To cite this version:**

Annette Calisti, Sandrine Ferri, Caroline Mossé, Bernard Talin, Annie Klisnick, et al.. Line Profiles of Ni-like Collisional XUV Laser Amplifiers: Particle Correlation Effects. High Energy Density Physics, 2013, 9, pp.516-522. 10.1016/j.hedp.2013.05.004 . hal-00720106v2

HAL Id: hal-00720106
https://hal.science/hal-00720106v2

Submitted on 4 Jun 2013

HAL is a multi-disciplinary open access archive for the deposit and dissemination of scientific research documents, whether they are published or not. The documents may come from teaching and research institutions in France or abroad, or from public or private research centers.

L'archive ouverte pluridisciplinaire **HAL**, est destinée au dépôt et à la diffusion de documents scientifiques de niveau recherche, publiés ou non, émanant des établissements d'enseignement et de recherche français ou étrangers, des laboratoires publics ou privés.

Line Profiles of Ni-like Collisional XUV Laser Amplifiers: Particle Correlation Effects

A. Calisti*, S. Ferri*, C. Mossé*, B. Talin*

PIIM, UMR7345, Aix-Marseille Université - CNRS, Campus Saint Jérôme, 13397 Marseille Cedex 20, France.

A. Klisnick*, L. Meng*

ISMO, UMR8214, Université Paris-Sud 11 - CNRS, Bat. 350, 91405 Orsay Cedex, France.

D. Benredjem*

LAC, UPR3321, CNRS, Université Paris-sud 11, 91405 Orsay, France.

O. Guilbaud*

LPGP, UMR8578, CNRS - Université Paris-Sud 11, Bat. 210, 91405 Orsay Cedex, France.

Abstract

We present a detailed analysis of the different processes that contribute to the spectral broadening of the Ni-like Ag XUV laser line, including the effects of particle correlations on the broadening due to the radiator motion (Doppler broadening). We consider two different regimes of collisional excitation pumping: the transient pumping for which ionic temperature is relatively low (the plasma coupling parameter is large), and the quasi steady-state pumping for which the ionic temperature is higher and the plasma coupling parameter is of the order of 1. In both cases, by using classical molecular dynamics simulation techniques, we show that ionic correlations actually modify the radiator-motion broadened profiles and cannot be neglected in evaluating the Doppler effect. The subsequent narrowing of the Doppler component is small compared to the overall linewidth, which includes the effect of homogeneous collisional broadening. However ionic correlations will also affect the amplification of the lasing line, especially when the laser enters the saturation regime, because it will lead to an homogenization of the spectral profile.

Keywords:
Line broadening, Homogeneous and inhomogeneous profiles, Ni-like Ag XUV laser line, Particle correlation effects

1. Introduction

There is an increasing interest in better understanding the spectral behaviour of plasma-based collisional XUV lasers in the last years [1, 2, 3, 4, 5]. The main reason is that the shortest pulse duration that was reached until now is limited to $\sim$ 1 picosecond [6] by the extremely narrow bandwidth of these sources. For numerous applications, like the production of plasma in the Warm Dense Matter regime (WDM) [7], one needs XUV lasers with a shorter pulse duration, namely in the subpicosecond or even in the femtosecond range. This could be obtained if the XUV laser is operated in an injection-seeded mode, using femtosecond high-order harmonic radiation as a seed [5, 6], but only on condition that the bandwidth be enlarged by a factor $\sim$ 3 or larger. The ultimate duration τ_{FL} of the output pulse of such an injection-seeded XUV laser is controlled by the spectral bandwidth of the plasma amplifier, through $\tau_{FL} \sim \frac{\lambda^2}{\Delta\lambda}$. The bandwidth that should be considered here involves not only the intrinsic (optically thin) broadening of

*Corresponding author
Email address: annette.calisti@univ-amu.fr (A. Calisti)

the lasing line, but also the effects of gain narrowing and potential saturation rebroadening occuring in the process of amplification, which depend on the degree of inhomogeneity of the intrinsic profile [8]. In order to define strategies to progress towards this goal, one needs to better characterize the respective contribution of the different broadening mechanisms that prevail in XUV laser plasmas.

The intrinsic spectral profile of emission lines in a plasma is determined predominantly by spontaneous emission rates, electron collisional rates, Stark broadening and Doppler broadening [9] with possible complications due to ion turbulence [10] and additional ion-ion interactions [10, 11, 12, 13]. In a medium with population inversions and gain, the observed profile is modified by radiative transport effects in being narrowed approximatively as the square root of the gain-length product in the small signal regime [8]. As the laser saturates, if the intrinsic profile is dominated by inhomogeneous rather than homogeneous broadening mechanisms, the line can be re-broadened to its intrinsic width. This points out clearly the importance of having a good representation of the intrinsic profile together with a good understanding of the different mechanisms responsible for broadening. It is usual to consider that the inhomogeneous broadening mechanisms are caused by the local inhomogeneities of the medium such as Doppler shifts, quasi-static electric microfields or turbulence and that homogeneous broadenings are mainly due to electron-radiator collisions and/or spontaneous emission. Nevertheless, similarly to the quasi-static electric field approximation which can be inappropriate in the Stark broadening theory due to perturber ion dynamics [14], the free particle formalism involved in the standard Doppler effect calculation could fail if ion velocities change over time scales of the same order of or shorter than the effective radiative lifetime of the oscillator (i.e. the inverse of homogeneous spectral linewidth). In other words, if the velocities change before the light emission happens, it is no longer possible to consider ions with straight trajectories and particle interactions have to be included in the calculation of the spectral profile. In some circumstances, the breakdown of the free particle approximation can have significant consequences in resulting in the narrowing of the intrinsic Doppler profile when the mean time of velocity-changing, t_c is shorter than the effective Doppler correlation time (Dicke narrowing [15]). On the other hand, when t_c is less than the effective radiative lifetime it can result in the effective homogenization of the ordinarily inhomogeneous Doppler profile by velocity redistribution, and affect the spectral and amplification behaviour at saturation.

In this paper we use a multi-electron radiator line broadening code, the PPP line shape code [16], to carry out a detailed analysis of the above broadening effects for the case of the XUV laser line emitted at $\lambda = 13.9$ nm, corresponding to the $4d - 4p$ ($J = 0 - 1$) transition in Ni-like Ag. Lasing at this wavelength can be achieved over a broad range of plasma density and temperatures, depending on the characteristics of the driving laser pulse, which is used to induce population inversions between the laser levels. Two pumping regimes were successfully implemented for XUV lasers and are considered in the present study. In the transient pumping regime [17], the free electrons are rapidly heated but the ionic temperature remains relatively low (around 20 eV) over the lasing timescale of few picoseconds. In the quasi-steady state (QSS) pumping regime [18], the longer lasing timescale ($\sim$ 100 ps) allows a more efficient thermalization of the ions with the heated electrons and the ionic temperature is higher (a few hundred eV). In both cases lasing is obtained over a relatively large range of electron density, around 10^{20} cm^{-3}. It is thus expected that the relative contribution of Doppler broadening and collisional broadening will substantially vary over the considered plasma parameter range. This range also corresponds to a strong coupling plasma regime where correlations between particles can no longer be ignored. We thus investigate the accuracy of the usual free-particle Doppler approximation, by using classical molecular dynamics (MD) simulations. We show that for both pumping regimes, ionic correlations actually modify the radiator-motion broadened profiles and cannot be neglected in evaluating the Doppler effect. Similar MD techniques were previously used in the context of XUV laser by Pollock et al. in 1993 [11] to study the existence of ionic correlation effects in Ne-like Se and Ni-like Ta pumped in the QSS regime. The authors concluded that collisional ("Dicke") narrowing was not a factor in modeling the studied XUV laser line shapes. Our present results, performed for a different element and over a broader plasma parameter range, are not in contradiction with these results. Although collisional narrowing induced by ionic correlations can be significant, especially at high electron density, the net effect remains relatively small, due to the important contribution of collisional broadening to the overall (intrinsic) linewidth. However we show that ionic correlations will lead to a significant homogenization of the spectral line that should be taken into account in the description of amplification and saturation of the lasing line. We propose a simple model that reproduces the results of the MD simulations with a good accuracy for the two considered regimes of pumping.

2. Spectral line shape modeling

If one accounts for the emitter motion, the general expression of the line profile reads [14]:

$$I(\omega) = \Re e \frac{1}{\pi} \int_0^\infty dt e^{i\omega t} < e^{i(\ \mathbf{k}\cdot\mathbf{r}(t) - \ \mathbf{k}\cdot\mathbf{r}(0))} \mathbf{d}(t) \cdot \mathbf{d}(0) > \tag{1}$$

where <> denotes an ensemble average over the emitter plus plasma system, $\mathbf{d}$ is the radiator dipole operator and $k = 2\pi/\lambda$ with λ the wavelength of the considered line. The factors $e^{\pm i\ \mathbf{k}\cdot\mathbf{r}}$ accounts for the radiator's center-of-mass motion. Broadenings due to the interaction of the emitting ion with surrounding particles and to emitter motion are statistically dependent in the general case. Broadening due to interactions results from a modification of the internal state of the atomic oscillator. Both this internal state and the velocity of translational motion of the emitter can be altered in the same collision.

In this study, interactions with the electronic component of the plasma dominate, giving rise to a phase shift of the atomic oscillator. This phase shift is due to electronic collisions which change substantially the phase without altering the velocity of the emitter owing to the great difference of masses. So, it is quite accurate to ignore correlations between the ion translation $\mathbf{r}(t)$ and the dipole moment $\mathbf{d}(t)$:

$$I(\omega) = \Re e \frac{1}{\pi} \int_0^\infty dt e^{i\omega t} < e^{i(\ \mathbf{k}\cdot\mathbf{r}(t) - \ \mathbf{k}\cdot\mathbf{r}(0))} >< \mathbf{d}(t) \cdot \mathbf{d}(0) > . \tag{2}$$

The line shape appears as the Fourier-transformed of a product of two correlation functions, the radiator dipole operator correlation function, $C(t) =< \mathbf{d}(t) \cdot \mathbf{d}(0) >$, and the self-structure factor, $S_s(k,t) =< e^{i(\ \mathbf{k}\cdot\mathbf{r}(t) - \ \mathbf{k}\cdot\mathbf{r}(0))} >$ which can be calculated independently. The line shape is also the convolution of the respective profiles due to interactions with the bath, $I_{int}(\omega)$ and to emitter motion $I_D(\omega)$.

The correlation function, $C(t)$, of the radiator dipole operator, $\mathbf{d}$ can be written in Liouville space as [19, 20]:

$$C(t) =\ll \mathbf{d}^\dagger | \{U_l(t)\}_{\text{bath}} | \mathbf{d}\rho_0 \gg \tag{3}$$

where the double bra and ket vectors are defined as usual in Liouville space. ρ_0 is the equilibrium density matrix and $\{U_l(t)\}_{\text{bath}}$ is the bath-averaged evolution operator of the emitter. $U_l(t)$ is solution of the following stochastic Liouville equation (SLE) :

$$\frac{dU_l(t)}{dt} = -iL_l.U_l(t) \tag{4}$$

with the condition $U(0) = I$. L_l designates the Liouvillian of the radiator in the bath. We have $L_l = L_0 + l(t)$, where L_0 is the Liouvillian of the free radiator and $l(t)$ a random perturbation of the thermal bath (the plasma).

In the standard theory [9, 14], due to their great difference of mass, ions and electrons are treated in different ways, leading to:

$$L_l(t) = L_0 - \mathbf{d} \cdot \mathbf{E_l}(t) - i\Phi \tag{5}$$

where $\mathbf{E_l}(t)$ is the electric field produced by surrounding ions in a given configuration l and Φ is the electronic collisional operator. The ionic electric field is usually considered as quasi-static and is represented by its static distribution $W(E_l)$ [21]. We then have

$$I_{int}(\omega) = \Re e \frac{1}{\pi} \int_0^\infty dt e^{i\omega t} \int_0^\infty dE_l W(E_l) \ll \mathbf{d}^\dagger | e^{-iL_l t} | \mathbf{d} \gg . \tag{6}$$

In this work, the PPP line shape code [16] is used to calculate $I_{int}(\omega)$. This code has been designed for calculating the profile of spectral lines emitted by multi-electron ionic emitters in hot and dense plasmas. The Stark broadening is taken into account in the framework of the standard theory by using the static ion approximation and an impact approximation for the electrons, or including the effects of ionic perturber dynamics by using the Fluctuation Frequency Model [22, 23] when the static approximation fails. The atomic data required for the calculation are extracted from an external atomic structure code [24]. The effect of the electronic microfield component on the radiator is calculated in the framework of a binary collision relaxation theory, introducing an homogeneous damping and shift

term, a collisional operator, to the emitter Hamiltonian. This operator depends on the density and temperature of the plasma and can be calculated either using a quantum mechanical relaxation theory or a classical path assumption for the perturbing electrons. Here, in the PPP code, the option of a modified semiclassical model, in which a strong (close) collision term is added to the semiclassical term, has been chosen [25].

The self-structure factor is well known in the free-particle limit resulting from the hypothesis that each radiating ion moves at constant velocity with a Maxwellian distribution of velocities, and is given by:

$$S_s(k,t) = e^{-k^2t^2/2\beta m}, \tag{7}$$

with $\beta = 1/k_BT$ and m the ion mass. A Fourier transform then yields the usual area-normalized Gaussian Doppler line profile:

$$I_D(\omega) = \frac{c}{\omega_0}\left[\frac{m}{2\pi k_BT}\right]^{1/2} exp\left[\frac{-mc^2(\omega-\omega_0)^2}{2k_BT\omega_0^2}\right] \tag{8}$$

with $\omega_0 = kc$, whose linewidth is given by:

$$\Delta\omega_D = 2\sqrt{\frac{2k_BT}{m}\ln 2} \times \frac{\omega_0}{c}. \tag{9}$$

A straightforward way to take into account interactions between ions in the calculation of the line shape, is to use a classical molecular dynamics simulation techniques (MD) to compute $S_s(k,t)$. A Fourier transform of $S_s(k,t)$ will yield the corresponding profile accounting for ionic interactions. In standard classical MD simulation, the plasma model consists of classical point ions interacting together through a coulombic potential screened by electrons and localized in a cubic box of side L with periodic boundary conditions. The ionic interaction potential is chosen to account for the polarization of the electron gas by the ionic charge distribution, with the screening length equals to the electron Debye length, $\lambda_D = \sqrt{\frac{k_BT_e}{4\pi N_e e^2}}$ in accordance with the plasma electronic densities, N_e, and temperatures, T_e. Newton's equations of particle motion are integrated by using a velocity-Verlet algorithm using a time-step consistent with energy conservation. Due to periodic boundary conditions, $k = 2\pi/\lambda$ must satisfy:

$$k_{x,y,z} = n_{x,y,z}2\pi/L, \tag{10}$$

$n_{x,y,z}$ being an integer number. The number of particules, N (thus L), is chosen to find k as close as possible to that of the considered laser line. Integrating the Newton's equation gives access to the positions and velocities of the ions as a function of time and thus to the associated static and dynamic statistical properties such as structure factors, velocity correlation functions, diffusion coefficients, ion-ion collision rates, etc.

3. Calculated linewidths

In this section, we investigate the broadening of the Ni-like Ag laser $4d - 4p$ ($J = 0 - 1$) line at 13.9 nm over a broad range of density and temperatures, over which collisional excitation pumping of this transition can be achieved. Electronic densities are in the range $5 \times 10^{19} - 8 \times 10^{20}$ cm^{-3}, the electron temperature can vary between 200 and 700 eV [26]. For the ionic temperature two different regimes of pumping were considered. For the transient pumping regime, the ionic temperature remains relatively low, typically 20 – 50 eV. For the quasi-steady state pumping regime, the ionic temperature is higher, typically 200 eV. The different causes of broadening (radiative decay, interaction with surrounding particles and Doppler effect) have been investigated over this extended plasma parameter range. In the following, we will discuss two series of results corresponding respectively to the transient pumping case ($T_i = 20$ eV, $T_e = 200$ eV) and to the QSS pumping case ($T_i = T_e = 200$ eV) pumping, for different electronic densities.

The PPP code was used to provide the optically thin spectral profile of the lines of interest for given values of density and temperature of the emitters and of the surrounding free electrons. It has been checked that the Stark effect associated with the ionic microfield has a negligible contribution to the line profile whatever the densities

and temperatures of interest. The homogeneous broadening consists in natural broadening and electronic collisional broadening. Accounting for both effects does not yield difficulties as they are statistically independent, giving rise to a line width equal to the sum of the respective line widths. In the following, this broadening will be referred to as lifetime broadening. The broadening due to the translational motion of the emitter (Doppler effect) has been obtained by using the self-structure factors computed by MD simulations, in order to account for velocity changing effects. The obtained linewidths were compared to the usual free-particle limit approximation (Eq. 9). Some typical numbers for the physical quantities of the simulated plasmas over the considered density range, and some technical details of the MD simulations are given in Table 1. The second and third columns show the values taken by the plasma coupling parameter $\Gamma = Z^2e^2/(r_0 kT_i)$, r_0 being the ion sphere radius, $r_0 = (3/(4\pi N_i))^{1/3}$, for the transient pumping case (trans) and for the QSS case respectively. One can see that in the transient case Γ takes large values, ranging between ~ 5 and ~ 14, while in the QSS case Γ is smaller, ranging between ~ 0.6 and ~ 1.4. As shown in Table 1 the number of particles, N, in the simulation box has been chosen equal to 300 for all conditions. This choice leads to a simulation box size L large compared to the correlation lengths ensuring the results to be independent of N while allowing to find k satisfying Eq. 10 and kr_0^{MD} matching the laser wave number $kr_0^{\rm laser}$. The remaining columns of Table 1 show the plasma frequency, $\omega_{\rm pi} = \sqrt{\dfrac{4\pi N_i (Z_i e)^2}{m}}$, and the Doppler frequency widths $\Delta\omega_D$ obtained in the free particle limit for the two considered pumping regimes.

N_e (cm^{-3})	$\Gamma_{\rm trans}$	$\Gamma_{\rm QSS}$	N	$kr_0^{\rm laser}$	$kr_0^{\rm MD}$	$\omega_{\rm pi}$ (eV)	$\Delta\omega_{\rm D}^{\rm trans}$ (eV)	$\Delta\omega_{\rm D}^{\rm QSS}$ (eV)
5×10^{19}	5.79	0.58	300	2.03	2.016	2.57×10^{-3}	2.95×10^{-3}	9.34×10^{-3}
1×10^{20}	7.29	0.73	300	1.61	1.647	3.64×10^{-3}	–	–
2×10^{20}	9.19	0.92	300	1.28	1.302	5.14×10^{-3}	–	–
4×10^{20}	11.57	1.16	300	1.01	1.008	7.27×10^{-3}	–	–
7×10^{20}	13.95	1.39	300	0.82	0.843	9.62×10^{-3}	–	–

Table 1: Some characteristic quantities used in MD simulations

Figure 1 shows the spectral linewidths (FWHM) obtained for the different broadening causes of the $4d-4p$ laser line calculated as a function of the electron density for the transient pumping case. Here, the ionic temperature is relatively low ($T_i = 20$ eV) and the electronic densities are in the range $5\times10^{19} - 7\times10^{20}$ cm^{-3}. The electron temperature is taken as $T_e = 200$ eV.

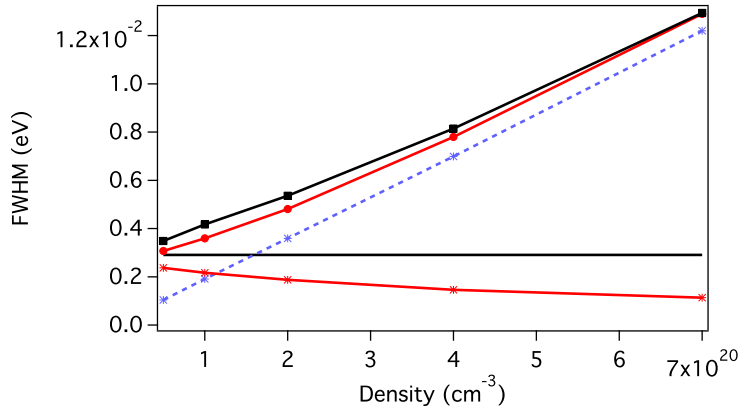

Figure 1: (Color online) Full-width at half-maximum spectral width versus density of the $4d-4p$ laser line in the transient pumping case. Dashed blue line and stars: Lifetime (radiative + collisional) broadening. Solid black line: Doppler (free-particle limit) broadening. Solid red line and stars: radiator motion broadening accounting for particle interactions. Upper curves: overall linewidth including all broadening contributions, in the free-particle limit (solid black line and squares), and accounting for interactions (solid red lines and circles).

One can see that the lifetime broadening (dashed blue and stars) increases almost linearly with the electron density, through the effect of electronic collisions. It becomes larger than the radiator motion broadening already at (relatively) low density, above $N_e \sim 1 - 2 \times 10^{20}$ cm^{-3}. The radiator motion broadening calculated in the free-particle limit (solid black) is compared to the results of MD simulations (solid red and stars), accounting for interactions between particles. In these cases, the plasmas are strongly coupled (Γ from $\sim$ 6 to $\sim$ 14) making the concept of binary collision between ions compromised because the ions are always in interaction with each others. Collective effects involving multiple collisions are expected to affect the profiles. Significant narrowing of the line induced by the effect of velocity changing is clearly seen over the entire considered range of electron density. When accounting for the contribution of lifetime broadening, the overall linewidth (upper curves) is less altered (compare black squares to red circles), especially towards high electron density where lifetime broadening dominates the profile. However it should be noted that the existence of significant particle correlations will also affect the line profile, in contributing to its homogenization, as will be discussed below.

For the QSS pumping case, the ionic temperature was taken equal to the electron temperature, $T_i = T_e = 200$ eV and four different electron densities were considered: $N_e = 1 \times 10^{20}, 2 \times 10^{20}, 4 \times 10^{20}$ and 7×10^{20} cm^{-3}. Because the ionic temperature is higher, the plasma coupling parameter in this regime is smaller than in the transient pumping case, ranging between 0.7 and 1.4 (see Table 1). The results of the PPP and MD simulations in terms of linewidth are shown in Fig. 2.

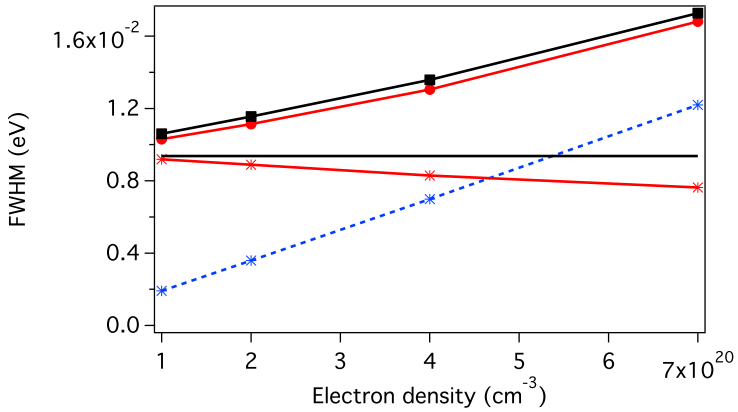

Figure 2: (Color online) Same as Fig.1 but for the QSS pumping regime.

As in the transient pumping case (Fig. 1), the lifetime broadening contribution increases linearly with N_e. However here it becomes dominant over the radiator motion broadening at large density only, typically above $5 - 6 \times 10^{20}$ cm^{-3}. This illustrates again the strong dependence of the contribution of lifetime broadening of the XUV laser intrinsic profile with respect to the local plasma parameters in the gain region. The narrowing of the radiator-motion linewidth induced by the correlations between particles is still clearly observed in Fig. 2, although it is smaller than in the transient pumping case (due to a smaller Γ). Finally this collisional narrowing is still apparent in the overall linewidth, even at high electron density, due to a comparatively smaller contribution of the lifetime broadening.

Similar results have been obtained for other electron temperatures (not shown in Figs 1 and 2). The contribution of the lifetime broadening to the intrinsic line profile has been calculated for different densities and for several electron temperatures up to 700 eV. The results were fitted with analytical functions and a simple expression was derived for the FWHM:

$$\Delta\lambda_{\rm h}(N_e, T_e) = \alpha_1 \times (kT_e)^{-\beta_1} \left(1 - \frac{N_e}{8{\times}10^{20}}\right) + \alpha_2 \times (kT_e)^{-\beta_2} \left(\frac{N_e}{8{\times}10^{19}} - 1\right) \tag{11}$$

where $\Delta\lambda_{\rm h}$ is in mÅ and N_e in cm^{-3}. The numerical values of the coefficients α_1, α_2, β_1 and β_2 derived from the fits are as follows: $\alpha_1 = 8.111 \times 10^{-3}$; $\alpha_2 = 8.533 \times 10^{-3}$; $\beta_1 = 0.2053$; $\beta_2 = 0.2373$. We have checked that

this formula reproduces the results of the detailed PPP calculations with an accuracy of better than ±2% within the explored range. This relation can be easily included in radiative transfer simulation codes, which require accurate values for the optically thin linewidth to calculate the spectral profile of the amplified XUV beam.

In the free-particle limit approximation, the (Doppler) line profile is inhomogeneous and can be described by a Gaussian function (Eq. 8). The Doppler linewidth depends on T_i only (Eq. 9). The lifetime broadening yields an homogeneous profile, which can be described by a Lorentzian function. As is well known, the resulting spectral profile will be the convolution of the homogeneous and inhomogeneous profiles, leading to the so-called Voigt profile. The overall linewidth, $\Delta\lambda_{tot}$, is a complex combination of both homogeneous, $\Delta\lambda_h$, and inhomogeneous, $\Delta\lambda_D$, linewidths. It has been checked that the formula derived in Ref. [27]:

$$\Delta\lambda_{tot} = \frac{1}{2}\Delta\lambda_h + (\frac{1}{4}\Delta\lambda_h^2 + \Delta\lambda_D^2)^{1/2} \tag{12}$$

fits our results to better than 1%.

It can be easily checked that the formula given by Eq. 12 does not fit our results if ionic interactions are taken into account. The ionic correlations do not only affect the linewidths but also induce an homogenization of the spectral profile. The radiator-motion profile is no longer Gaussian, and the overall profile is no longer a Voigt profile. Not only Eq. 12 no longer applies, but the relative weight of homogeneous versus inhomogeneous components in the overall intrinsic profile, which controls its behavior at saturation, is significantly modified. It is thus necessary to investigate in more detail the modification induced to the spectral profile by the effect of velocity-changing collisions. This is the purpose of the next section.

4. CALCULATED SPECTRAL PROFILES

In this section, we will focus our discussion on the radiator motion broadening component, ignoring the contribution of the lifetime broadening to the spectral profile.

The narrowing of the radiator-motion profile, observed for both the transient and QSS pumping regime (Figs. 1 and 2), can be understood in terms of the correlation function $S_s(k,t)$ for a moving emitter. In the free particle limit, $S_s(k,t) = e^{-k^2t^2/2\beta m} \equiv e^{-k^2t^2\overline{v}^2/4}$, the characteristic Doppler correlation time is $\tau_D \approx \lambda/\overline{v}$. τ_D can then be understood as the time taken by a radiator having the mean thermal velocity $\overline{v}$ to move a distance equal to the laser emission line λ. Any factor restricting or hindering the movement of the emitter will broaden $S_s(k,t)$ and hence narrow the line shape. Due to the strong coupling plasma parameters involved here (in particular in the transient pumping case), ions are in constant interaction and they are more and more hindered to move freely as the plasma density (or the coupling factor Γ) increases.

For a better understanding of the effect of these long range interactions, line profiles calculated for different densities are plotted in the same graph in logarithmic units, for two ionic temperatures corresponding to the transient (Fig.3(a), T_i = 20 eV) and QSS (Fig.3(b), T_i = 200 eV) pumping regimes respectively. In both graphs the unaffected Doppler profile is also plotted for comparison. It can be seen that the effect of ionic correlations yields distinct features in the profile in each pumping regime. In the transient pumping case (Fig.3(a)) the profile is not only narrowed but a shoulder structure appears in the wings, at a distance form the line center that increases with N_e. In the QSS pumping case (Fig.3(b)), the line shape is modified and the width is slightly reduced, but no structures are apparent in the wings. The frequency shifts, $\Delta\omega_{\rm osc}$, delimiting the position of the shoulders are shown by black arrows in Fig.3(a). We have checked that the values of those frequency shifts are actually close to the ionic plasma frequency for the given N_e. More precisely they correspond to the oscillation frequency of the velocity autocorrelation function, $C_v(t) =< \mathbf{v}(t)\cdot\mathbf{v}(0) >$. This function reveals the properties of single-particle motion in the plasma. $C_v(t)$ is calculated from our MD simulations and the oscillation frequency, $\Delta\omega_{\rm osc}$ is deduced from $C_v(t)$ by a Fourier transform. Examples of calculated velocity autocorrelation functions and of their Fourier transforms are given in Fig.4(a) and Fig.4(b), for several values of Γ. For the largest values of Γ the decay of $C_v(t)$ is characterized by the appearance at large times of oscillations at a frequency close to $\omega_{\rm pi}$. The oscillations are already seen at Γ = 5.786 ($N_e = 5\times10^{19}$ cm^{-3}) and become more pronounced as Γ increases. They are due to the coupling between the collective density fluctuations and the single particle motion [28].

In order to have a more detailed insight into the dynamics of a particle in those XUV laser plasmas, we have calculated the evolution in time of the frequency distribution associated to a set of particles chosen to have an initial

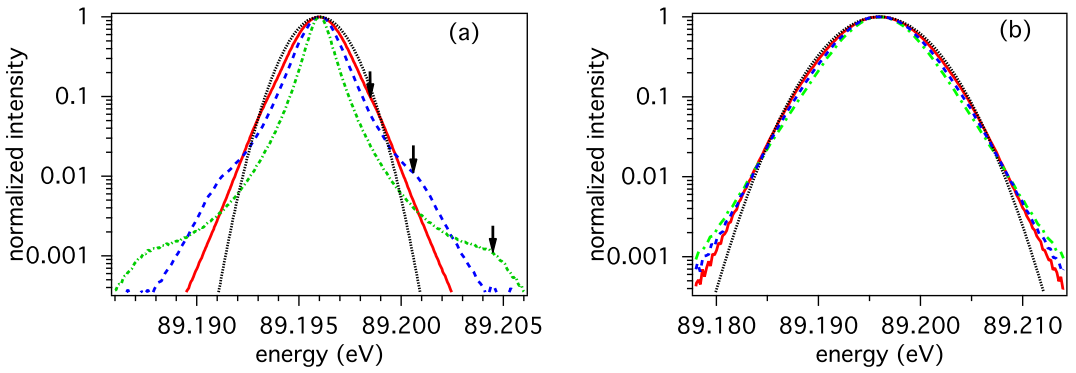

Figure 3: (Color online) Spectral profile of the $4d - 4p$ laser line including the radiation-motion broadening in the presence of ionic correlations for 3 different electron densities. (a) Transient pumping case, $T_i = 20$ eV; (b) QSS pumping case, $T_i = 200$ eV. Red solid line: $N_e = 5 \times 10^{19}$ cm^{-3} in (a) and $N_e = 1 \times 10^{20}$ cm^{-3} in (b). Blue dashed line: $N_e = 2 \times 10^{20}$ cm^{-3}. Green dash-dot line: $N_e = 7 \times 10^{20}$ cm^{-3} . Black dotted line: Doppler profile in the free-particle limit. In (a) the black arrows show the positions of the shoulder structures, which are given by the oscillation frequency of the velocity autocorrelation function.

velocity $\mathbf{v}(0)$ such as $\mathbf{k} \cdot \mathbf{v}(0) = \omega \pm \Delta\omega$ for $\omega = 0$ and $\Delta\omega$ chosen sufficiently large to have a representative number of tagged particles. The plasma conditions are those relevant to the QSS pumping case at $N_e = 1 \times 10^{20}$ cm^{-3}, i.e. conditions where the plasma coupling parameter is not large ($\Gamma = 0.73$), and collisional narrowing is small (see Fig.2). The results of the calculation are shown in Fig.5. The sharper distribution corresponds to the initial time when the set of particles such as $\mathbf{k} \cdot \mathbf{v}(0) = 0$ emit at a frequency equals to $\omega_0 \pm \Delta\omega$. As time increases the frequency distribution gets broader, as a result of velocity-changing collisions, and tends to the infinite time limit corresponding to a frequency distribution given by the equilibrium velocity distribution. This limit is the usual Doppler distribution in the free-particle limit, also shown in Fig.5 (black dashed curve). Four different times of evolution (0.24 ω_{pi}^{-1}, ω_{pi}^{-1}, 2.5 ω_{pi}^{-1} and 3.83 ω_{pi}^{-1}) have been chosen, the latter corresponding to the radiative lifetime of the laser transition. It can thus be seen that during their effective lifetime, the radiating and absorbing ions sample many velocities, not just one as it is supposed in the Doppler free particle limit. The effect of this rapid velocity redistribution will be to effectively homogenize the radiator-motion broadening component of the intrinsic line profile. Similar effect is also obtained for conditions relevant to the transient pumping case. This means that collisional redistribution cannot be ignored when evaluating the spectral behaviour of the laser line following amplification and saturation.

An interesting feature that can be noticed in Fig.5 is that interactions between particles give rise to small changes in the velocity at short time-scale: the frequency redistribution at $t = 0.24\ \omega_{\rm pi}^{-1}$ is limited to frequencies around the initial frequency suggesting that the interactions give rise to small-angle scattering. Moreover, it is necessary to wait long enough to fill the entire distribution. This behavior suggests that the dynamics of the ions in the present plasmas could be modeled by a Brownian-movement model [13, 29]. In this model, the following expression was derived for the self-structure factor:

$$S_s(k,t) = e^{-\frac{k^2}{2}<x_k^2>}, < x_k^2 >= \frac{\bar{v}^2}{\nu_d^2}(\nu_d t - 1 - e^{-\nu_d t}) \tag{13}$$

where $< x_k^2 >$ is the mean square displacement in the direction of k over the time t and $\bar{v} = \sqrt{2k_B T_i/m}$. It is shown in [29] that ν_d is related to $C_v(t)$ by:

$$C_v(t) \equiv < \mathbf{v}(t) \cdot \mathbf{v}(0) >= \frac{3}{2}\bar{v}e^{-\nu_d t}. \tag{14}$$

The values of ν_d have been obtained by fitting the velocity autocorrelation functions obtained from our MD simulations (see e.g. Fig4) with an exponential decreasing function. The ν_d values have been used in Eq. 13 to calculate $S_s(k,t)$, from which the line profile was derived through a Fourier transform. The results are presented in Fig.6 and compared with our detailed MD calculations.

It can be seen in Fig.6 that the Brownian-movement model gives a very good approximation to the spectral profiles

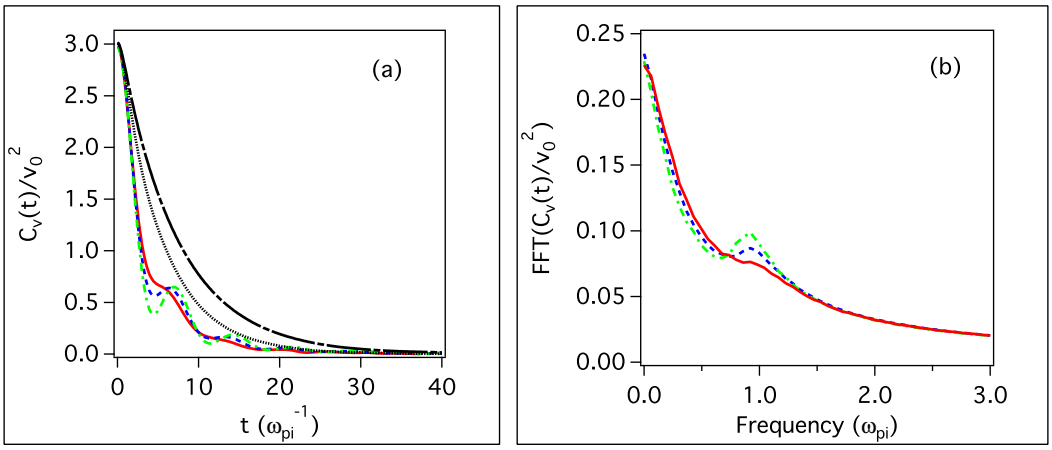

Figure 4: (Color online) (a) Velocity autocorrelation function $C_v(t)$ for increasing values of the coupling factor Γ. Black dash-dot line: $\Gamma = 0.73$. Black dotted line: $\Gamma = 1.39$. Solid red line: $\Gamma = 5.79$. Blue dashed line: $\Gamma = 9.19$. Green dash-dot green line: $\Gamma = 13.95$. (b) Fourier transform of $C_v(t)$ for $\Gamma = 5.79$, 9.19 and 13.95 (same color code). The velocities are in units of $\sqrt{kT_i/m}$ and the time in units of $\omega_{\rm pi}^{-1}$.

calculated from detailed MD simulations, for both transient and QSS pumping cases and over a broad range of electron density, even though the wings and the shoulder structures are not reproduced correctly. This is mainly because the velocity autocorrelation function, $C_v(t)$, can be very far from an exponential decreasing function, as it can be seen in Fig.4. Fitting $C_v(t)$ by an exponential form eliminates the oscillations expected at a frequency near ω_{pi}. Moreover the Markovian approximation used in the Brownian-movement model (e.g. any memory associated with the motion of the particle is ignored) is not valid in the plasmas of interest here, where the diffusing particles are similar to their neighbors [29]. Nevertheless, the Brownian-movement model without memory proposed here provides a simple and rapid way to account for the homogenization of the laser line profile due to ionic correlations, in good agreement with more sophisticated MD simulations. Such a model could be easily implemented in a radiative transfer calculation to investigate the saturation behaviour of the laser line in the transient and QSS pumping regime.

5. Conclusion

In this paper we have presented a detailed analysis of the different broadening processes that affect the intrinsic profile of a XUV laser line, over an extended range of plasma parameters. Such a study is important to clarify the prospects of extending the duration of existing collisional XUV lasers towards shorter femtosecond duration, since this duration is currently limited by the extremely narrow bandwidth. Two different regimes of collisional excitation pumping have been considered: transient pumping for which ionic temperature is relatively low, so the plasma coupling parameter is large, and quasi steady state pumping for which the ionic temperature is higher and the plasma coupling parameter is of the order of 1. We show that the relative contribution of the lifetime broadening to the overall line profile strongly depends on the local plasma parameters in the lasing plasma. Using molecular dynamics simulations we have investigated the effect of ionic correlations on the radiator-motion broadening component. We find that, for all the plasma parameter range explored, this effect cannot be ignored. We show that ionic correlations lead to a significant narrowing of the radiator-motion broadened component compared to the usual Doppler (free-particle) limit, especially in the (low ionic temperature) transient pumping case. However this effect is largely masked when accounting for the lifetime broadening in the overall linewidth. We show that ionic correlations will also affect the inhomogeneous nature and, to a lesser extent, the shape of the profile, which are both important in evaluating the behaviour of the laser line through amplification and saturation. By investigating the velocity autocorrelation function we show that the spectral features observed in the radiator-motion broadened profile are related to the plasma ionic oscillations. Finally we propose to use the Brownian-movement model to calculate the self-structure factor and the radiator-motion broadened line profile. This study will be the scope of our future work.

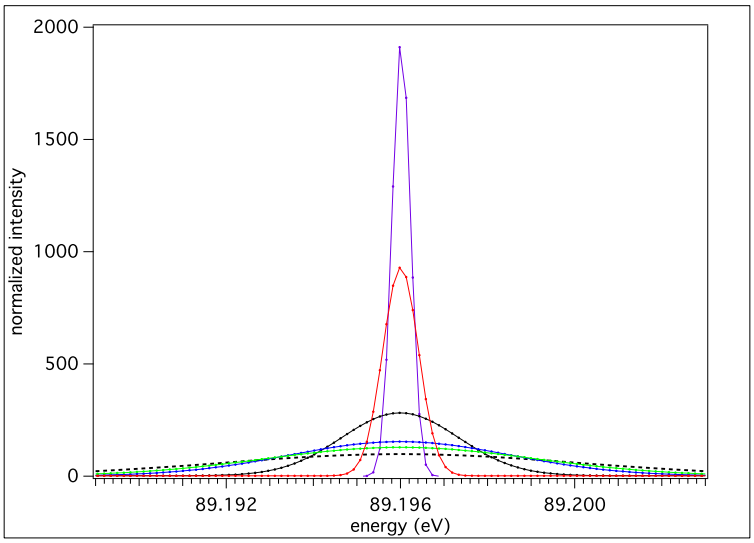

Figure 5: (Color online) Evolution with time of the frequency distribution function of a set of particles with an initial velocity such as $\mathbf{k}\cdot\mathbf{v}(0) = 0\pm\Delta\omega$ for plasma conditions relevant to the QSS pumping case at $N_e = 1\times10^{20}$ cm^{-3}. Times $t = 0$ (purple), 0.24 $\omega_{\rm pi}^{-1}$ (red), ω_{pi}^{-1} (black), 2.5 ω_{pi}^{-1} (blue) and 3.83 ω_{pi}^{-1} (green). The frequency distribution gets broader with time, on a timescale that is comparable with the radiative lifetime. The black dash line corresponds to the Doppler free-particle limit that would be reached at infinite time.

[1] O. Guilbaud, A. Klisnick, D. Joyeux, D. Benredjem, K. Cassou, S. Kazamias, D. Ros, D. Phalippou, G. Jamelot and C. Möller, Eur. Phys. J. D. 40 125 (2006).
[2] D. Benredjem, C. Möller, J. Dubau and T. Ball, Phys. Rev. A 73 063820 (2006).
[3] O. Guilbaud, F. Tissandier, J.-P. Goddet, M. Ribière, S. Sebban, J. Gautier, D. Joyeux, D. Ros, K. Cassou, S. Kazamias, A. Klisnick, J. Habib, Ph. Zeitoun, D. Benredjem, T. Mocek, J. Nedjl, D. de Rossi, G. Maynard, B. Cros, A. Boudaa and A. Calisti, Opt. Lett. 35 1326 (2010).
[4] F. Tissandier, S. Sebban, M. Ribière, J. Gautier, Ph. Zeitoun, G. Lambert, A. Barszczak Sardinha, J.-Ph. Goddet, F. Burgy, T. Lefrou, C. Valentin, A. Rousse, O. Guilbaud, A. Klisnick, J. Nejdl, T. Mocek, G. Maynard, Phys. Rev. A 81 063833 (2010).
[5] D. S. Whittaker, M. Fajardo, Ph. Zeitoun, J. Gautier, E. Oliva, S. Sebban and P. Velarde, Phys. Rev. A 81 043836 (2010).
[6] Y. Wang, M. Berrill, F. Pedaci, M. M. Shakya, S. Gilbertson, Z. Chang, E. Granados, B. M. Luther, M. A. Larotonda, J. J. Rocca, Phys. Rev. A 79 023810 (2009).
[7] U. Zastrau, C. Fortmann, R. R. Faustlin, L. F. Cao, T. Doppner, S. Dusterer, S. H. Glenzer, G. Gregori, T. Laarmann, H. J. Lee, A. Przystawik, P. Radcliffe, H. Reinholz, G. Ropke, R. Thiele, J. Tiggesbaumker, N. X. Truong, S. Toleikis, I. Uschmann, A. Wierling, T. Tschentscher, E. Forster and R. Redmer, Phys. Rev. E 78 066406 (2008).
[8] G. J. Pert, JOSA B **11**, 1425 (1994).
[9] H.R. Griem, *Spectral line broadening by plasmas*, (Academic, New York, 1974).
[10] H.R. Griem, Phys. rev. A **33**, 3580 (1986).
[11] E.L. Pollock and R. A. London, Phys. Fluids B **5**, 4495 (1993).
[12] J.A. Koch et al., Phys. Rev. A **50**, 1877 (1994).
[13] S.G. Rautian and I.I Sobel'man, Usp. Fiz. Nauk **90**, 209 (1966).
[14] H.R. Griem, *Principles of Plasma Spectroscopy*, (Cambridge University Press, 1997).
[15] R.H. Dicke, Phys. Rev. **89**, 472 (1953).
[16] A. Calisti, F. Khelfaoui, R. Stamm, B. Talin, and R. W. Lee, Phys. Rev A **42**, 5433 (1990).
[17] A. Klisnick, P. Zeitoun, D. Ros, A. Carillon, P. Fourcade, S. Hubert, G. Jamelot, C.L.S. Lewis, A. G. Mac Phee, R.M.N. O'Rourcke, R. Keenan, P. V. Nickles, K. Janulewicz, M. Kalashnikov, J. Warwick, J.-C. Chanteloup, A. Migus, E. Salmon, C. Sauteret, and J.P. Zou, Journal of the Optical Society of America B **17**, 1093 (2000).
[18] J. Zhang, A.G. MacPhee, J. Nilsen, J. Lin, T.W. Barbee, Jr., C. Danson, M.H. Key, C.L.S. Lewis, D. Neely, R.M.N. O'Rourke, G.J. Pert, R. Smith, G.J. Tallents, J.S. Wark, and E. Wolfrum, Physical Review Letters **78**, 3856 (1997).
[19] M. Baranger, *Atomic and Molecular Processes*, edited by D.R. Bates (Academic, New York, 1964).
[20] U. Fano, Phys. Rev. **131**, 259 (1963).
[21] C.A. Iglesias, H.E. DeWitt, J.L. Lebowitz, D. MacGowan, and W.B. Hubbard, Phys. Rev. A **31**, 1698 (1985); C.A. Iglesias, et al., J. Quant. Spectrosc. Radiat. Transf. **65**, 303 (2000).
[22] B. Talin, A. Calisti, L. Godbert, R. Stamm, R.W. Lee and L. Klein, Phys. Rev. A **51**, 1918 (1995).
[23] A. Calisti et al., Phys Rev. E **81**, 016406 (2010).

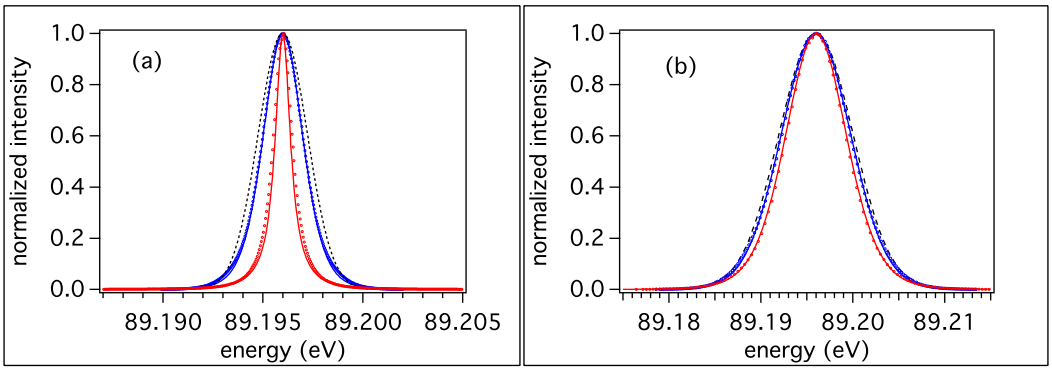

Figure 6: (Color online) Spectral profile (radiator motion broadening component) of the $4d - 4p$ laser line line calculated using the Brownian-movement model to account for ionic correlation effects. (a) Transient pumping: $N_e = 5 \times 10^{19}$ (solid blue); $N_e = 7 \times 10^{20}$ (solid red). (b) QSS pumping: $N_e = 1 \times 10^{20}$ (solid blue); $N_e = 7 \times 10^{20}$ (solid red). Our model reproduces very well the detailed MD simulation results (dotted lines). The black dotted curve corresponds to the usual Doppler profile in the free-particle limit.

[24] I.P. Grant et al., Comput. Phys. Commun. **21**, 207 (1980).
[25] H.R. Griem, M. Blaha and P.C. Kepple, Phys. Rev. A **19**, 2421 (1979).
[26] G.J. Pert, Physical Review A **73**, 033809 (2006).
[27] T.J. Manning, J.D. Winefordner, B.A. Palmer, D.E. Hof, Acta Part B **45**, 1031 (1990).
[28] J.P. Hansen, I. R McDonald and E.L. Pollock, Phys. Rev. A **11**, 1025 (1975).
[29] J.P. Hansen and I. R McDonald, *Theory of Simple Liquids*, (Academic Press, London, 1976).